Appl. Phys. B 66, 759–764 (1998)

Applied Physics B
Lasers
and Optics

Subthreshold tunable OPO: a source of nonclassical light for atomic physics experiments

E.S. Polzik, J.L. Sørensen, J. Hald

Institute of Physics and Astronomy, Aarhus University, 8000 Aarhus c, Denmark

Received: 11 March 1998/Revised version: 1 April 1998

Abstract. The frequency-tunable subthreshold OPO has become a unique source for probing and driving atoms with nonclassical light. Applications span from sub-shot-noise atomic measurements to proposals for the generation of quantum-correlated atomic ensembles. We briefly review the experiments performed to date and then concentrate on the recent results in atomic spin polarization experiments with nonclassical OPO light.

PACS: 42.50Dv; 42.50Lc; 42.65Yj

A subthreshold optical parametric oscillator does not, in fact, oscillate in a sense of generating a nonzero mean field. Rather, it amplifies the vacuum electromagnetic field converting it into resonator enhanced spontaneous parametric emission. As a result of such a nonoscillatory regime, the subthreshold OPO (sub-OPO) can simultaneously emit many modes without mode competition, which complicates the stable performance of above-threshold OPOs. This feature proves crucial in applications of the sub-OPO in atomic physics and spectroscopy where the continuous frequency tunability is a must. The sub-OPO emits light in a whole set of modes, which are symmetrically positioned in the frequency domain around the degeneracy frequency $\omega_0 = \omega_{\text{pump}}/2$. If the phase-matching conditions are chosen to correspond to the near-degenerate regime, all the modes are normally in resonance with the cavity provided the central degenerate mode is resonant. Therefore tuning of such an OPO can be achieved by just tuning ω_0 and keeping the cavity in resonance with this frequency. If a particular application requires the OPO to be operated at nondegenerate phase-matching conditions the three equations $\omega_+ + \omega_- = 2\omega_0$, $n\lambda_- = L$, and $m\lambda_+ = L$ (m and n integers), which establish the resonance for the two parametric frequencies, are not necessarily obeyed. Nonetheless, even in this case tuning is much easier than for the above-threshold OPO. Just by changing the cavity length L one can achieve the required simultaneous resonance. Such relatively straightforward tunability makes the nonclassical light generated by the sub-OPO readily available for atomic physics and spectroscopy applications.

A remarkable feature of the sub-OPO output, which lays the foundation for the applications described in this paper, is the strong nonclassical correlation between the OPO output fields, $a(\omega_+)$ and $a(\omega_-)$, at the two symmetric frequencies ω_+ and ω_-. This can be characterized by the correlation function $\langle a(\omega_+)a(\omega_-)\rangle = M\delta(2\omega_0 - \omega_+ - \omega_-)$ [1]. For the lossless sub-OPO one obtains $|M|^2 = N^2 + N$, where N is the photon number spectral density at frequencies $\omega_\pm$, defined as $\langle a^\dagger(\omega_\pm)a(\omega')\rangle = N\delta(\omega_\pm - \omega')$. For classical states of light one finds $|M|^2 \leqslant N^2$, and therefore it is the presence of the N term in $|M|^2$, which is characteristic for the manifestly nonclassical behavior. Since the output noise of the sub-OPO is Gaussian, all its properties can be expressed through the second-order correlation functions, M and N. For a single-ended lossless sub-OPO $N = 4x/(x-1)^2$ where $x = P/P_{\text{th}}$ is the dimensionless pump power of the OPO.

In the first application of the sub-OPO in atomic spectroscopy [2] the OPO output has been mixed with a coherent local oscillator (LO) and used as a passive probe for the FM spectroscopy of an atomic vapor. The quantum noise of such a squeezed probe can be expressed in terms of the quadrature phase amplitude of the OPO output $X(\varphi) = (1/\sqrt{2})[(a_+ + a_-)\,\mathrm{e}^{\mathrm{i}\varphi} + (a_+^\dagger + a_-^\dagger)\,\mathrm{e}^{-\mathrm{i}\varphi}]$ ($X(\varphi) = a_+\,\mathrm{e}^{\mathrm{i}\varphi} + a_+^\dagger\,\mathrm{e}^{-i\varphi}$ for the degenerate OPO), where φ is the phase of the OPO output with regard to the LO. The probe noise normalized to the shot-noise level is then given by $\langle \delta X^2(\varphi)\rangle = 1 + 2N + 2\,|M|\cos(2\varphi + \psi)$, where we have defined ψ to be the argument of M. For $2\varphi + \psi = \pi$ and for the OPO operating close to the threshold, meaning that ($x \to 1$), we find $\langle \delta X^2(\varphi)\rangle \to 0$. This allows for the sub-shot-noise, in principle noiseless, atomic spectroscopy. In practice, different kinds of losses restricted the quantum noise reduction achieved in [2] to -3.8 dB, which corresponds to the lowering of the noise level to about 42% of the original shot noise level.

The next series of experiments [3, 4] used the sub-OPO output (squeezed vacuum) in a completely different way, namely to drive a two-photon transition in an atom. The probability of the two-photon excitation can be expressed as $P_2 \propto \alpha\,|M|^2 + N^2$ with α as a constant depending on the parameters of the atom [5]. However, independent of the particular

atomic system, in the case of excitation with the squeezed vacuum from the OPO, we find $P_2 \propto \alpha N + (\alpha+1)N^2$. This implies that for small photon numbers, N, the two-photon excitation probability goes linearly with the intensity of the excitation. This manifestly nonclassical dynamics of an atom driven with nonclassical light has been experimentally demonstrated in [3]. The pictorial explanation of this effect can be given by visualizing the sub-OPO output as a flux of photon pairs with just the right phase link as to satisfy the two-photon excitation condition (again due to the nature of the correlation function M).

1 Nonclassical light in atomic spin polarization experiments

1.1 Sub-shot-noise polarization spectroscopy of cold atoms

The frequency-tunable sub-OPO can be also used to generate polarization-squeezed light to perform atomic sub-shot-noise polarization spectroscopy in a polarization interferometer. As demonstrated experimentally in [6], when a linearly polarized coherent field is mixed with an orthogonally polarized squeezed vacuum, the noise level in a polarization interferometer can drop below the shot-noise level. This property of the polarization interferometer can be used for sub-shot-noise atomic polarimetry as demonstrated below, but only if the atomic medium is optically thin. For an optically thick atomic ensemble, absorption of the probe together with quantum atomic spin noise generally precludes sub-shot-noise observations, as demonstrated in [7].

Our polarization interferometer consists of two polarizers rotated 45° relative to each other by means of a half-wave retarder ($\lambda/2$) as shown in Fig. 1. The first polarizer PBS1 serves to clean the vertical polarization of the coherent part of the probe and as a port for mixing in squeezed vacuum. The second polarizer PBS2 splits the coherent probe onto two photodiodes (PD1/2), the radio frequency (rf) components of the photocurrents are subtracted in a 180° rf combiner, and the result is analyzed with an rf spectrum analyzer (SA). With

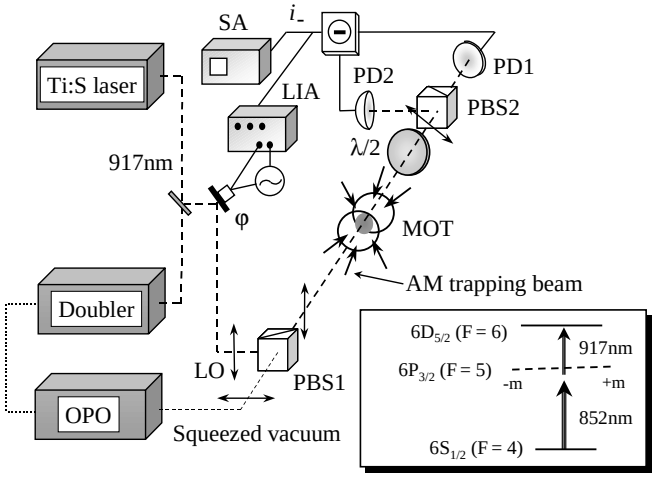

Fig. 1. The atomic polarization spectroscopy setup with a squeezed probe. The signal is recorded on the spectrum analyser (SA), and the phase φ is optimised using the lock-in amplifier (LIA). The insert shows the atomic levels of interest

no optically active medium between the two polarizers, the photocurrents from PD1 and PD2 are balanced, so that ideally after subtraction nothing but the incoherent quantum noise of the probe is left to be detected. If, however, an anisotropic medium is placed between the polarizers, the polarization of the linearly polarized probe rotates by an angle θ, and the photocurrents of the two photodiodes differ by the amount $i_- = 2\theta i_0$. Here i_0 is the total photocurrent coming from both PDs. We assume here a detector quantum efficiency of 1, meaning that i_0 describes the photon flux incident on each detector as well as the photocurrent in units of the elementary charge. As a result of the imbalance in the detection caused by the finite θ, i_- will now contain a contribution due to the atomic noise as well as the probe shot noise. It can be shown that in the case of the shot-noise-limited probe this setup gives the same signal-to-noise ratio as the more conventional polarization interferometer with nearly 90° crossed polarizers [8]. However, even when the polarization is not rotated, our detectors are still exposed to the light. From a technical viewpoint this means that our measurement precision is limited by the optical noise (shot noise) in contrast to the electronic noise for the crossed polarizer setup. Furthermore all the probe light reaches the detectors in our setup. This is of vital importance when the probe is squeezed, since any loss of light from a squeezed field will limit the quantum-noise reduction.

The rotation angle can be shown to have two contributions [9]. The first one comes from the circular birefringence arising from different indices of refraction experienced by the σ^+ and σ^- components of the linearly polarized probe. This results in a phase shift between the two components, as they emerge from the anisotropic medium, and consequently a rotation of the polarization. The other contribution comes from the difference in the extinction coefficients for the light polarized at $+45°$ and at $-45°$ relative to the horizontal axis, this is commonly called the linear dichroism. We can now write the rotation angle to the lowest order in the differences as

$$\theta_{\text{signal}} = \pi \frac{\ell}{\lambda} (n_+ - n_-) + \frac{1}{2} \ell \, (\alpha_{+45} - \alpha_{-45}) \,, \tag{1}$$

where $n_\pm$ are the indices of refraction for the $\sigma^\pm$ polarized light, and $\alpha_{\pm 45}$ are the extinction coefficients for the light polarized at $\pm 45°$ relative to the horizontal axis. λ is the wavelength of the probe and ℓ is the length of the region of interaction.

The anisotropic medium used in our experiment is a sample of about 10^6 ^{133}Cs atoms, trapped and cooled to about 100 μK in a magneto-optical trap (MOT). We employ the three-level ladder transition $6S_{1/2}(F=4) \rightarrow 6P_{3/2}(F=5) \rightarrow 6D_{5/2}(F=6)$ as illustrated in Fig. 1. The atoms are trapped on the lower transition (852 nm), and the deviation from a uniform distribution of the populations of the $6P_{3/2}(F=5)$ magnetic sublevels is probed on the upper transition (917 nm). For trapping we use a diode laser stabilized with an external grating and locked to the $6S_{1/2}(F=4) \rightarrow 6P_{3/2}(F=5)$ transition. In order to produce good squeezing in the probe at 917 nm we need a laser with small technical fluctuations, and hence we use a Ti:sapphire laser for this purpose. On the two-photon resonance the absorption and consequently the second contribution in (1) is expected to dominate, whereas off resonance the phase shift in the first term of (1) will dominate in the observed signal.

In order to avoid the contamination of our signals from the low-frequency technical noise, the measurement is performed at an rf frequency of $\Omega/2\pi = 3\,\mathrm{MHz}$. The atomic signal is generated by intensity modulating one trapping beam at the frequency $\Omega/2\pi$, causing a modulation of the atomic populations at the same frequency. The ac part of the differential photocurrent can be written as

$$\delta i_-^2 = 4i_0^2\delta\theta^2 + 4\theta^2\delta i_0^2 \simeq 4i_0^2\delta\theta^2 . \quad (2)$$

Here we neglect the second term, which comes from the amplitude noise of the probe, assuming that θ is small and/or a quiet laser is used. The first term in (2) contains several contributions:

$$\delta i_-^2 = 4i_0^2\delta\theta^2 = 4i_0^2\left(\delta\theta^2_{\text{signal}} + \delta\theta^2_{\text{probe noise}} + \delta\theta^2_{\text{spin noise}}\right) . \quad (3)$$

The first term in (3) is our signal, which is due to the modulation of the atomic parameters in (1). The second term is due to the quantum noise of the polarization of the probe. The third term is due to the spin noise of the atomic sample. This term is relevant for an optically thick medium [7] and can therefore be omitted in the present section, where the optical depth of the probed atoms is low. In the next section we discuss theoretically how this term becomes important when the optical depth is appreciable. In this case a squeezed probe will not enhance the signal-to-noise ratio. Instead, driving the $6S_{1/2}(F=4) \rightarrow 6P_{3/2}(F=5)$ transition with squeezed light may turn out to be fruitful.

Concentrating on the probe quantum noise $4i_0^2\delta\theta^2_{\text{probe noise}}$ for now, we note that our photocurrent i_- is given by the intensity difference between the light polarized at $+45°$ and the light polarized at $-45°$ relative to the horizontal axis of PBS1. Thus i_- corresponds, in our dimensionless units, to the expectation value of the Stokes operator $S_2 = \alpha_y^\dagger c_x + c_x^\dagger \alpha_y = \alpha_y X(\varphi)$, where α_y is the vertically polarized coherent field chosen to be real. $c_x = a\,\mathrm{e}^{\mathrm{i}\varphi}$ is the horizontally polarized squeezed vacuum emerging from PBS1 [10], a is the field emerging from the sub-OPO, and $X(\varphi)$ is the quadrature of the field a in-phase with the coherent field. The angular polarization noise can be expressed as $\delta\theta^2_{\text{probe noise}} = \langle\delta X^2(\varphi)\rangle/(4\left|\alpha_y\right|^2) = \langle\delta X^2(\varphi)\rangle/(4i_0)$, where we have used that $i_0 = \left|\alpha_y\right|^2$, and

$$\begin{aligned}\left(\delta i_-^2\right)_{\text{probe noise}} &= \left\langle\delta S_2^2\right\rangle = 4i_0^2\delta\theta^2_{\text{probe noise}} = i_0\left\langle\delta X^2(\varphi)\right\rangle \\ &= i_0(1+2N+2\left|M\right|\cos[2\varphi+\psi]) = i_0(1-\zeta) . \end{aligned} \quad (4)$$

For the OPO close to the threshold and $2\varphi+\psi=\pi$, the angular polarization uncertainty and the probe quantum noise are suppressed by the factor $(1-\zeta)$ (last equality), where ζ is the degree of squeezing ($\zeta \rightarrow 1$ for an ideal OPO close to the threshold). The operator complementary to S_2 is $S_3 = -i(\alpha_y^\dagger c_x - c_x^\dagger \alpha_y)$, which describes the degree of ellipticity of the polarization of the field. When the fluctuations in S_2 are reduced below the standard quantum limit, the fluctuations of S_3 are increased, since S_2 and S_3 must obey the Heisenberg uncertainty relation

$$\left\langle\delta S_2^2\right\rangle\left\langle\delta S_3^2\right\rangle \geq i_0^2 . \quad (5)$$

This means that by mixing the squeezed vacuum with the coherent state on PBS1, we create a field with a very well defined polarization angle at the expense of a strongly fluctuating ellipticity of the polarization. By phase shifting squeezed vacuum with regard to the coherent component either the S_2 or S_3 Stokes parameter can be squeezed. For our polarization interferometer this will result in a probe with reduced or increased quantum noise, respectively.

We now turn to the atomic contribution to our signal. From (3) we find that it is given by $4i_0^2\delta\theta^2_{\text{signal}}$. According to (1) it consists of two terms: one arising from the modulation of the indices of refraction and another arising from the modulated absorption. As the probe is scanned across the atomic resonance, the index of refraction, and hence the difference between the indices of refraction, varies like the derivative of a Lorentzian, whereas the absorption varies like a Lorentzian. The intensity modulation of a trapping beam will cause amplitude modulation of these signals. Consequently the recorded noise power of the photocurrent at the modulation frequency will vary like the square of the sum of the above mentioned shapes [11]. Now we can write up the output of the SA as

$$\begin{aligned} S(\Omega) &= 2i_0 B\,(1-\zeta) \\ &\quad + 4i_0^2\left(\xi_1\frac{\Delta\Gamma}{\Delta^2+\Gamma^2/4} + \xi_2\frac{\Gamma^2/4}{\Delta^2+\Gamma^2/4}\right)^2 . \end{aligned} \quad (6)$$

Here B is the rf bandwidth of the SA, Δ is the probe detuning from atomic resonance, Γ is the FWHM of the atomic transition, and ξ_1 and ξ_2 are parameters containing the information on the strength of the modulation and depending on the efficiency of the modulation transfer from the trapping beams to the probe via the trapped atoms. It has been assumed that the atomic sample is optically thin, so that no appreciable amount of probe light is absorbed when it passes through the trap. Furthermore we have used that the external modulation of the atoms has a bandwidth much smaller than B.

The probe light driving the polarization interferometer and our squeezed light source is provided by a Microlase MBR-110 Ti:sapphire laser operating at 917 nm. As illustrated in Fig. 1 about 600 mW of optical power from this laser pumps a nonlinear optical cavity containing a $KNbO_3$ crystal to produce the second harmonic with about 75% efficiency. The second harmonic is used to pump another nonlinear $KNbO_3$ cavity operated as a subthreshold OPO. The OPO acts as the source of squeezed vacuum in our experiment. The latter is mixed on PBS1 with a coherent beam split off the Ti:sapphire output before the doubling cavity. We obtain the desired polarization squeezed state by adjusting the relative phase between the two fields to be $(\pi-\psi)/2$ as required by (4). In practice the phase is locked by analyzing the noise power of the photocurrent i_- at a frequency about 100 kHz away from $\Omega/2\pi$, where no modulation noise from the spectroscopic signal is present. A voltage proportional to the noise power is produced, and by using a standard dither and lock technique, φ is stabilized to minimize the noise.

The degree of the quantum-noise reduction in our experiment is limited by the following factors. Not all of the OPO intracavity photons escape through the output coupler; in fact only 85% comes out this way, limiting the observable squeezing to the same value. Our measurement has a finite bandwidth, meaning that we do not wait forever for both photons in each correlated pair to escape the OPO cavity. Consequently we lose another 6% of squeezing. Our propagation losses are 10% and the homodyne efficiency on PBS1 is 98%. All in all we end up with 3.6 dB of quantum noise reduction.

However, when the LO phase is locked to the minimum quantum noise we lose another 0.6 dB of squeezing, resulting in 3 dB of squeezing being available for the atomic polarization spectroscopy. The quantum noise of the probe in the absence of atoms with the LO phase scanned and locked is shown in Fig. 2. Our best squeezing with this setup is 5 dB, as reported in [12], but, possibly because of the high phase-matching temperature for a-cut $KNbO_3$ at 917 nm, these fragile crystals have deteriorated in time. As a result, the nonlinearity has decreased and with the maximum pumping power available we can reach a gain of only about 6.5 dB, which, along with the factors listed above, results in 3 dB of observable quantum-noise reduction in the polarization interferometer.

With the MOT trapping laser turned on, a sample of cold atoms is formed in the path of the probe, and we observe the spectroscopic signal (6) on the SA as we scan the Ti:sapphire frequency across the resonance. The SA traces are shown in Fig. 3. By first blocking the squeezed OPO output we found that the signal peaked 2.3 dB above the shot-noise level. This corresponds to a signal-to-noise ratio of 0.7. By unblocking the squeezed vacuum we find that the noise floor limiting the measurement is reduced down to 2.5 dB below the shot-noise level, corresponding to a value of $\zeta = 0.44$ in (6). Since the atomic signal size stays almost unchanged, we have increased the signal-to-noise ratio of the measurement to 1.5 by employing the polarization-squeezed state in our polarization interferometer. Ideally the improvement in signal-to-noise ratio of 2.1 times should correspond to $(1-\zeta)^{-1}$, but because of fluctuations in the atomic signal, these two numbers differ somewhat. By adapting our theory (6) to the traces in Fig. 3, using that the rf bandwidth is $B = 100$ kHz, we can infer the parameters $2i_0\xi_1^2 = (63 \pm 5)$kHz and $\xi_2/\xi_1 = (36 \pm 2)\%$ for this particular trap configuration. Obviously the index of refraction of the trapped atoms is more efficient in transferring the modulation from the trapping beam to the probe than the absorption is. This is probably due to the geometry of the experiment, where the modulated σ^+ polarized trapping beam propagates at an angle of about 20° relative to the probe. As a result we have almost perfect symmetry between the modulated extinction coefficients $\alpha_{\pm 45}$. In contrast to this,

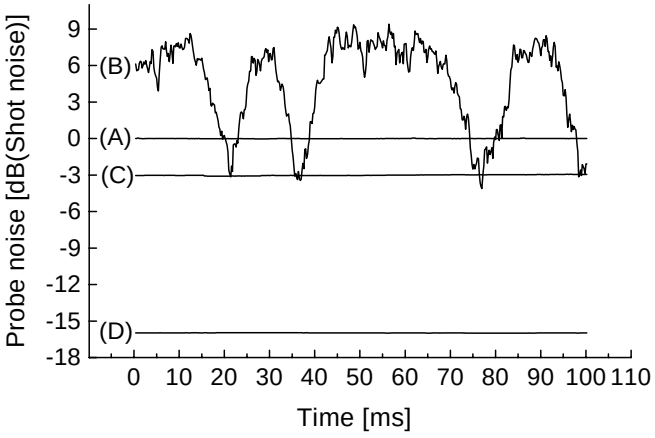

Fig. 2. Probe noise in units of the shot noise level (A) when the LO phase is scanned (B) and locked (C). The electronic noise (D) is shown to be 16 dB below the shot noise. The trace was taken with 1.5 mW of probe power, and the phase was scanned at a 17 Hz repetition rate

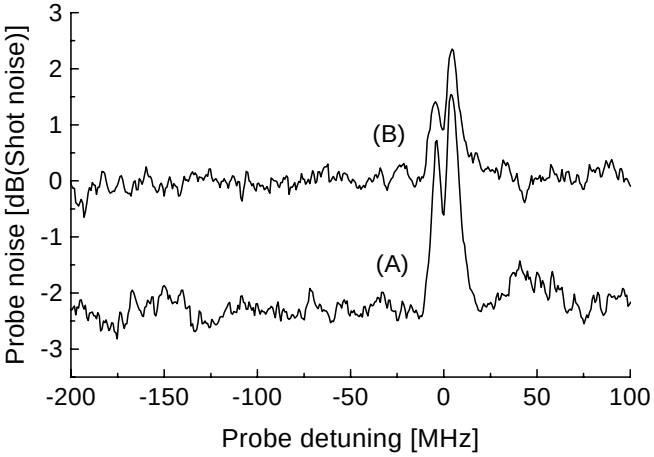

Fig. 3. Polarisation spectroscopy with a polarisation squeezed probe (A) and with the probe in a coherent state (B)

the indices of refraction for $\sigma^{\pm}$ polarized light, $n_{\pm}$, are modulated very differently.

1.2 From quantum correlations of light to quantum correlations of atomic spins

The promising future the sub-OPO offers in atomic physics is due to the fact that the two quantum correlated fields a_+ and a_- can interact with two different atoms and therefore introduce nonclassical correlations between these atoms. This observation has led to a proposal of generating spin squeezed states (SSS) of an atomic ensemble via an interaction with the sub-OPO output [13], as well as, in a more general sense, to new possibilities of creating quantum-correlated atomic ensembles.

In this section we outline the strategy for generation and detection of SSS in a Cs MOT. Consider an atomic ensemble with the atoms initially in the state $|g, m_g = 0\rangle$ where m_g is the magnetic quantum number (Fig. 4). If the atomic ensemble is excited with two quantum-correlated fields, A and B, along the two possible paths of the V-type configuration, it is reasonable to expect that some degree of quantum correlation will be transferred to the atoms in the final states $|e, m_e = -1, 1\rangle$. That this effect is a two-atom effect is obvious from the following consideration. A single-atom interaction rate in a V-type system involves either "trivial" correlation functions $\langle A^\dagger A\rangle, \langle B^\dagger B\rangle$ or "nontrivial" functions $\langle A^\dagger B\rangle, \langle B^\dagger A\rangle$. However, the latter nontrivial functions are zero for the OPO output, and therefore do not cause notable single-atom effects. The situation changes significantly when an ensemble of atoms is considered and multi-atom correlations are taken into account. Towards this end let us introduce the collective continuous spin operator of the excited state in the following way. The collective continuous density matrix element of the excited state $\sigma_{ij}(z,t)$ is defined as $\sigma_{ij}(z,t) = (1/\varrho\delta V)\sum_\mu \exp\left[i\omega_{ij}c(z-z_\mu)/c\right]\sigma_{ij}^\mu$ [14] where $\sigma_{ij}^\mu = |i\rangle\langle j|, (i, j \in \{-1, 1\})$ for μth atom, ω_{ij} is the frequency splitting between the two upper substates, z is the axis along which the light is propagating, and ϱ is the atomic density. The density matrix element has been normalized to the number of atoms, $\varrho\delta V$, in the volume element of interest, δV. For atomic samples of the laboratory size and

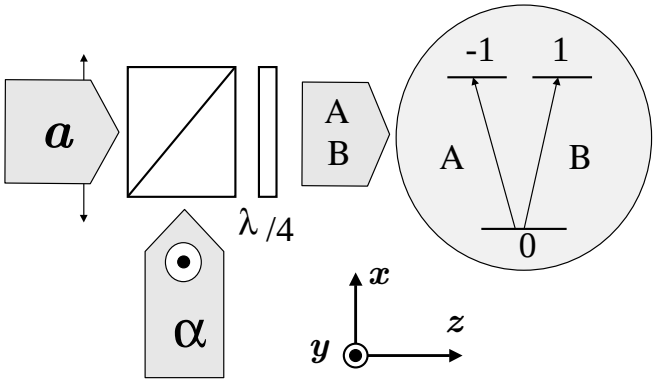

Fig. 4. Mapping of non-classical light onto an ensemble of V-type atoms. Coherent field a and squeezed vacuum α in two orthogonal polarizations are mixed on a polarizing beamsplitter. The quarter wave retarder serves to form the squeezed σ^- polarized field A and the coherent σ^+ polarized field B, which interact with the two arms of the V transition

ω_{ij} in the MHz range the exponent can be substituted by unity. The spin (quasi-spin) components of the excited state are then $J_z = (\sigma_{-1,-1} - \sigma_{1,1})/2$, $J_x = (\sigma_{-1,1} + \sigma_{1,-1})/2$, $J_y = -i(\sigma_{-1,1} - \sigma_{1,-1})/2$. Suppose now that the fields A and B are prepared by mixing a coherent state α and the sub-OPO output a in the orthogonal polarization on a polarizing beam splitter (Fig. 4). After the $\lambda/4$ plate the polarization of the coherent (squeezed vacuum) component becomes left-hand (right-hand) circular. In the lowest-order perturbation theory one then obtains

$$
\begin{aligned}
&J_z \propto \alpha\alpha^*,\\
&J_y \propto \alpha(a + a^+) \propto X(\varphi = 0),\\
&J_x \propto \alpha(a - a^+) \propto X(\varphi = \frac{\pi}{2}).
\end{aligned}
\tag{7}
$$

In the above we omitted the subscripts $+, -$ of the field operators, assuming that the frequencies of the correlated fields are almost equal (nearly degenerate OPO). Equations (7) tell us that the mean spin is oriented along the z axis, since this is the only component with nonzero mean. This is natural given that the coherent light is circularly polarized. The transverse components $J_{x,y}$ have zero mean and their variances are $\langle \delta J^2_{x,y} \rangle \propto \langle \delta X^2(\varphi) \rangle$. For the sub-OPO output one of the quadrature phase amplitudes has a variance less than that for the vacuum field. This means that one of the transverse collective spin components has its variance less than the pure coherent spin state, which corresponds to the excitation with only circularly polarized coherent light. Such a spin state is called a squeezed spin state [15, 16]. The above-described process of SSS generation with squeezed light from the sub-OPO has its physical origin in mapping of the pairwise photon correlations of light onto atoms. As a result the atoms also acquire pairwise correlations in their spin-polarization components. It has been shown in [13] that the process of spontaneous emission from the upper states partly destroys quantum correlations between the atoms. However, in the steady state 50% of those correlations survive under the condition of complete absorption of the sub-OPO output in the atomic medium.

In the above, SSS are generated for atoms in the final states of the transitions driven by quantum-correlated excitation. To observe it we need to address only these atoms in our measurement procedure. This is exactly what occurs in the process of a quantum-limited polarization-noise measurement, similar to the one described in [7]. We will now outline how the SSS can be detected via a polarization-noise measurement of cold Cs atoms. For Cs, level 0 can be the extreme sub-level of the ground state $m = F = 4$, and levels $-1, 1$ are sub-levels $m = 3, 5$ of the $6P_{3/2}$, $F' = 5$ excited state. The trapping light on this transition (see the previous section) has to be chopped, and the quantum-correlated excitation with the coherent and squeezed vacuum beams turned on during the "dark" periods when the measurements are taken. Excitation from magnetic sublevels other than $m = 4$ of the ground state can be avoided with a suitable optical pre-pumping. To measure, e.g., J_y in the $6P_{3/2}$, $F' = 5$ excited state, a linearly polarized probe resonant with the $6P_{3/2}$, $F' = 5 \rightarrow 6D_{5/2}$, $F' = 6$ transition, as in the previous section, is analyzed with a polarizing beam splitter oriented at 45° relative to the x axis, rendering the intensities $i(+45°)$ and $i(-45°)$. For the resonant probe $i_- = i(+45°) - i(-45°) = \alpha i_0 \Gamma J_y$ [17], where α is a constant proportional to the optical depth of the medium, i_0 is the probe intensity and Γ is the width of the transition. Obviously, quantum noise of i_- is determined by the quantum noise of J_y. When no squeezed vacuum is present, a certain spin noise level proportional to the square root of the number of atoms is present on the top of the shot noise of the probe as observed in [7]. When the squeezed vacuum with an appropriate phase is present, J_y should become squeezed and this noise level should drop below the level set by the coherent spin-state fluctuations demonstrating the SSS of the atomic ensemble.

2 Summary

The subthreshold tunable OPO has become a powerful tool for the atomic physics and spectroscopy with the nonclassical light. The quantum-correlated output of this device has been demonstrated to cause a manifestly quantum behavior of driven three-level atoms, as well as to allow standard quantum limits to be overcome in atomic absorption and polarization spectroscopy.

New perspectives in atomic physics with nonclassical OPO light appeared when it was realized that the OPO quantum-correlated output can be efficiently mapped onto optically thick atomic ensembles. The experiment on the preparation and observation of the so-called spin squeezed states, the first proposal to generate nonclassical collective atomic spin states with the nonclassical light, is currently in preparation in our laboratory. Further possibilities include production of the entangled atoms utilizing the Einstein–Podolsky–Rosen (EPR) correlations in the output of the nondegenerate OPO.

Whereas the first proposals deal with the generation of atomic correlations in excited states, the OPO output can, in principle, be used to produce entanglement of long-living atomic states populated via Raman-type processes. Such systems may prove well suited to enter quantum computation schemes and to serve for quantum key distribution in quantum cryptography.

Acknowledgements. This research has been supported by the Danish Research Council.

References

1. C.W. Gardiner: Phys. Rev. Lett. **56**, 1917 (1986)
2. E.S. Polzik, J. Carri, H.J. Kimble: Phys. Rev. Lett. **68**, 3020 (1992); Appl. Phys. B **55**, 189 (1992)
3. N. Georgiades, E.S. Polzik, K. Edamatsu, H.J. Kimble, A.S. Parkins: Phys. Rev. Lett. **75**, 3426 (1995); see also Z. Ficek, P.D. Drummond, Phys. Today **50**, 34 (1997)
4. N. Georgiades, E.S. Polzik, H.J. Kimble: Phys. Rev. A **55**, R1605 (1997)
5. J. Geo-Banacloche: Phys. Rev. Lett. 62, 1603 (1989); J. Javanainen, P.L. Gould: Phys. Rev. A **41**, 5088 (1990); Z. Ficek, P.D. Drummond: Phys. Rev. A **43**, 6247, 6258 (1992)
6. P. Grangier, R.E. Slusher, B. Yurke, A. LaPorta: Phys. Rev. Lett. **59**, 2153 (1987)
7. J.L. Sørensen, J. Hald, E.S. Polzik: Phys. Rev. Lett. **80**, 3487 (1998)
8. C. Wieman, T.W. Hansch: Phys. Rev. Lett. **36**, 1170 (1976)
9. A. Weis, J. Wurster, S.I. Kanorsky: J. Opt. Soc. Am. B **10**, 716 (1993)
10. R. Tanas, S. Kielich: J. Mod. Opt. **37**, 1935 (1990)
11. J.L. Sørensen, J. Hald, E.S. Polzik: Opt. Lett. **23**, 25 (1998)
12. J.L. Sørensen, J. Hald, N. Jørgensen, J. Erland, E. S. Polzik: Quantum Semiclass. Opt. **9**, 239 (1997)
13. A. Kuzmich, K. Mølmer, E.S. Polzik: Phys. Rev. Lett. **79**, 4782 (1997)
14. M. Fleichhauer, T. Richter: Phys. Rev. A **31**, 3761 (1985)
15. M. Kitagawa, M. Ueda: Phys. Rev.A **47**, 5138 (1993)
16. D.J. Wineland, J.J. Bollinger, W.M. Itano, D.J. Heinzen: Phys. Rev. A **50**, 67 (1994)
17. C. Cohen-Tannoudji, F. Laloe: J. Physique **28**, 505 (1967); F. Laloe, M. Leduc, P. Minguzzi: J. Physique **30**, 277 (1969)